Spin Crossover

International Edition: DOI: 10.1002/anie.201509294
German Edition: DOI: 10.1002/ange.201509294

Reversible Control by Light of the High-Spin Low-Spin Elastic Interface inside the Bistable Region of a Robust Spin-Transition Single Crystal

*Mouhamadou Sy, Damien Garrot, Ahmed Slimani, Miguel Páez-Espejo, François Varret, and Kamel Boukheddaden**

Abstract: *By using a weak modulated laser intensity we have succeeded in reversibly controlling the dynamics of the spin-crossover (SC) single crystal [{Fe(NCSe)(py)$_2$}$_2$(m-bpypz)] inside the thermal hysteresis. The experiment could be repeated several times with a reproducible response of the high-spin low-spin interface and without crystal damage. In-depth investigations as a function of the amplitude and frequency of the excitation brought to light the existence of a cut-off frequency ca. 1.5 Hz. The results not only document the applicability of SC materials as actuators, memory devices, or switches, but also open a new avenue for the reversible photo-control of the spin transition inside the thermal hysteresis.*

The control of the dynamics of first-order phase transitions is a very general and appealing problem in a diversity of fields. It concerns the irreversible character of the processes involved and makes their control of very high importance from the fundamental point of view and also for technological applications. Thus, systems showing propagating-interface phenomena include fluid invasion in porous media, flame fronts, cracks, domain wall in ferroic materials. Although very different, their microscopic descriptions share very similar physics at the macroscopic scale and can be described under a unifying framework involving competitions between elasticity and pinning by disordered medium. In cooperative spin-crossover solids,[1–4] the thermally induced first-order transition involves two spin states, namely the low-spin (LS, diamagnetic) and the high-spin (HS, paramagnetic) and is accompanied by a sizeable volume change and thermal hysteresis loop. For comparison, in magnetic systems, the control of the interface between ferromagnetic and paramagnetic domains is made possible thanks to the magnetic field, which induces the domain-wall motion,[5–7] which may be reversible under some conditions owing to the presence of the demagnetizing field created by the dipolar magnetic interactions. Such a control by a field parameter is no longer possible in spin-crossover solids, since the macroscopic interfaces separating the LS and HS states are elastic in nature. Axial pressure might act as an efficient control parameter; however its practical realization faces serious challenges, such as the brittle nature of the spin-crossover single crystals.[8–10] Among the promising multifunctional materials, multiferroic systems are of note, these are studied as a route to harness magneto-electric coupling and enable a range of applications whereby magnetism (resp. ferroelectricity) can be controlled by an electric (resp. magnetic) field.[11–13] Interestingly, multiferroic Jahn–Teller switches have been already reported for Prussian Blue analogues[14–16] demonstrating the important role of the elastic interactions in the control of the electronic properties of SC solids. But elasticity is also at the heart of many other types of phase transitions, such as in the Mott metal–insulator transition[17] where it has been shown that the coupling to crystal elasticity alters the critical properties.

Using optical microscopy investigations,[9,10,18,19] we shown that by tuning the shining intensity of the microscope, in the hysteretic region of the spin transition (see Figure 1), the temperature of the crystal was efficiently shifted and we could drive the interface position at will between the HS and the LS phases. However, this preliminary experiment remained qualitative. Herein, we show for the first-time how we can achieve an accurate and reversible control of the SC transition inside the hysteretic region. For that, we implemented a new experimental setup, in which the illumination of the sample is made by a laser beam injected through the objective of the microscope (see Supporting Information). A laser spot of approximately 8 μm diameter is then formed at the surface of the crystal (see Figure 1 b) the intensity of which is modulated using a function generator (see Supporting Information for the technical details).

The sample was a single crystal (length × width × thickness $\approx 120 \times 15 \times 10\ \mu m^3$) of the SC compound [{Fe(NCSe)(py)$_2$}$_2$-(*m*-bpypz)] where py = pyridine and bpypz = 3,5-bis(2-pyridyl)pyrazolate,[20,21] abbreviated herein as Fe(NCSe)(py)$_2$, undergoing a thermal first-order transition with hysteresis between 108.1 K and 114.5 K (see Figure 1 a). This crystal is very robust and presents an exceptional resilience upon repeated switching.[8] The experimental procedure was as follows: First, we prepared the crystal in the LS state, inside the thermal hysteresis loop (see Ref. [18]), at 112.5 K under a weak intensity of the microscope $I \approx 2.4\ mW\,cm^{-2}$ with the laser switched off. In the second step, we gradually increased

[*] M. Sy, Dr. D. Garrot, M. Páez-Espejo, Prof. Dr. F. Varret, Prof. Dr. K. Boukheddaden
Groupe d'Etudes de la Matière Condensée
CNRS-Université de Versailles; Université Paris Saclay
45 Avenue des Etats Unis, 78035 Versailles Cedex (France)
E-mail: kbo@physique.uvsq.fr
Dr. A. Slimani
Laboratoire des Matériaux Ferroélectriques, Département de Physique, Faculté des Sciences de Sfax
Route de Soukra km 3.5 BP 1171, 3018 SFax (Tunisia)

Supporting information for this article is available on the WWW under http://dx.doi.org/10.1002/anie.201509294.

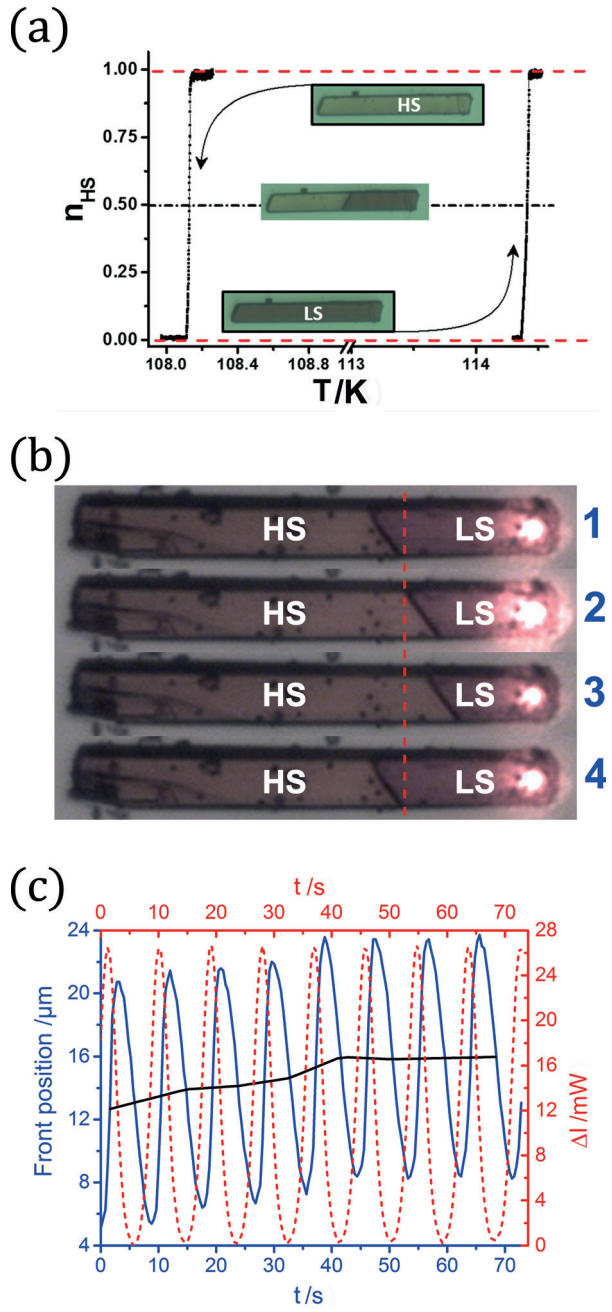

Figure 1. a) Thermal evolution of the HS fraction, n_{HS}, derived from optical microscopy measurements of Fe(NCSe)(py)$_2$ showing the hysteresis region. Inset: optical microscopy images of a single crystal in the LS (bottom), the HS (top) and in the biphasic (middle) states. b): Selected snapshots of the photo-control of the interface motion for different intensity values, (1–4 correspond to the times $t = 9.2$, 10.8, 12.4, and 18 s, respectively. See the complete spatiotemporal evolution in Supporting Information, movie S1. The vertical broken red line is given as a reference to locate the interface position). Bright dot on right hand side in each image is the laser light. c): Time dependence of the excitation (dotted red line) and the interface's position (solid blue line). The black curve shows the average "equilibrium" position of the HS/LS interface.

the intensity of the microscope lamp, until generating the nucleation of a macroscopic HS phase (by photo-heating). Then, we quickly decreased the light intensity so as to stop the interface motion, and the crystal was left in a stable biphasic state. In the final step, we modulated (at controlled frequency) the intensity of the laser spot, placed at an extremity of the crystal, in the LS phase (see Figure 1b), and we followed the interface response.

In Figure 1b, we selected a few snapshots of the crystal during periodic illumination at a frequency of 0.1 Hz. The complete spatiotemporal behavior is shown in the Supporting Information (movie S1). The pictures taken at times, 9.2 s, 10.8 s, 12.4 s, 18 s from top to bottom, reveal the stability of orientation of the HS/LS interface during the motion. Figure 1c shows the time evolution of excitation $\Delta I(t)$ (dotted red line) and the response of the interface position, $\Delta X(t)$ (full blue line), obtained after image processing of movie S1, the details of which are given in Figure S1 and S2 of the Supporting Information. Two points can be noted. First, the HS/LS interface performs periodic oscillations (the same applies for the HS fraction $\propto \Delta X(t)$) at the excitation frequency ($\nu = 0.1$ Hz), with a delay $\Delta t \approx 5$ s. The maximum velocity measured for the front propagation (which depends on temperature) was approximately 10 µm s^{-1} and corresponded to the "natural" growth of the HS phase under the usual warming experiment at 0.2 K min^{-1}. Second, a global drift of the average interface position (black curve of Figure 1c) appears in the beginning of the process before reaching a new stationary value around 40 s later. This behavior merely results from the heating effect of the shining process. These features are also well illustrated by the phase portrait $\Delta X(t)$ versus $\Delta I(t)$, given in Figure S3, showing an elliptic behavior, recalling the Lissajous curves used to characterize phase shifts.[22,23]

Now, we turn to the energetic aspects of the problem. When the amplitude of the laser excitation, ΔI_{max} (at fixed frequency) is increased, the photo-heating effect increases, resulting in a linear variation of the front excursion amplitude, ΔX_{max}, with ΔI_{max} (Figure S4), with a yield $\frac{\Delta X_{max}}{\Delta I_{max}} \approx 0.87(\pm 0.08)$ µm mW^{-1} which is at least one order of magnitude larger than for photo-control methods based on pulsed laser excitations, already reported.[24–27] We also carried out experiments at various frequencies of modulation, the results of which are displayed in Figure 2. At low frequencies, the excitation efficiently heats the crystal and drives the front

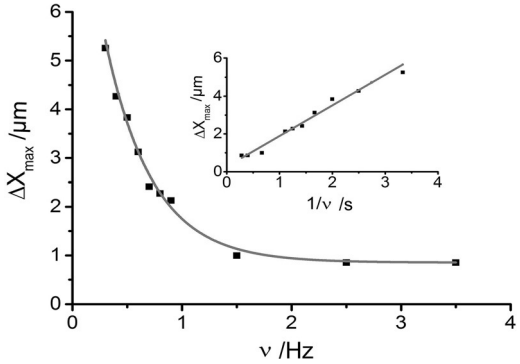

Figure 2. Excursion amplitude of the HS/LS interface of Fe(NCSe)(py)$_2$ as function of the frequency (black squares). Inset: ΔX_{max} vs. $1/\nu$ showing a linear behavior. The intensity of the light modulation was varied in the interval 0.518–4.86 mW. Solid lines are to guide the eye.

oscillations with large excursion amplitudes, ΔX_{max}. We have roughly estimated (see Supporting Information) the temperature increase to be approximately 5 K under illumination at 1 Hz. As depicted in inset of Figure 2, the measured ΔX_{max} linearly depends on $^1/_\nu$. This confirms that the ΔX_{max} is proportional to the quantity of heat $\Delta Q_{in} = \frac{1}{\nu} \cdot a_{LS} \cdot \Delta I_{max}$, absorbed by the material, the temperature of which rises by $\frac{\Delta Q_{in}}{C_p}$, where C_p is the heat capacity of the material. For higher ν values, we observed the existence of a cut-off frequency, $\nu_c \approx 1.5$ Hz ($2\Pi/\omega_c \approx 0.66$ s), above which the HS/LS interface is no longer able to follow the light excitation signal. Indeed, for $\nu > \nu_c$, the average amount of heat deposited by the laser spot during the time needed for heat exchange and diffusion (between 1 and 2.5 seconds) is not sufficient to heat efficiently the crystal

For a detailed understanding of the previous observations, we developed a model in which we accounted for all relevant contributions (schematized in Figure S6) including photoheating, thermal diffusion, heat-transfer processes, and spin-transition dynamics. The equations of motion governing this phenomenon, can be described by Equations (1)–(3).

$$\begin{cases} \frac{\partial m}{\partial t} = \Gamma J[-m + tanh\,\beta(Jm - \Delta_{eff})] + D_m \times \Delta m & (1) \\ C_p \frac{\partial T}{\partial t} = -\alpha C_p (T - T_B) + I\left(1 + (\rho - 1)\frac{1+m}{2}\right) + C_p D_T \times \Delta T & (2) \\ I(x,y,t) = I_0 + \frac{\Delta I_{max}}{2\pi\sigma}(1 - cos(\omega t))exp\left[-\frac{(x-x_0)^2 + (y-y_0)^2}{\sigma^2}\right] & (3) \end{cases}$$

Equation (1) is derived from an expansion of the mean-field free energy of an Ising-like model[28] about power gradients of the HS fraction.[29] It expresses the spatiotemporal behavior of the SC transition. There, m is the net "fictitious" magnetization ($-1 \le m \le +1$) related to the HS fraction by $n_{HS} = (1+m)/2$, $J = 155$ K is the interaction parameter between the spin states of the Ising-like model, $\beta = \frac{1}{k_B T}$ (k_B = Boltzmann constant and T = temperature), $\Delta_{eff} = \Delta - \frac{1}{2} k_B T \ln g$ is the effective energy gap which includes the ligand-field energy $\Delta = 394$ K and the degeneracy ratio $g = 1097$ between the HS and LS states (corresponding entropy change $S \approx 58$ J Mol^{-1} K^{-1}), and $D_m = 120$ μm^2 s^{-1} is the effective diffusion parameter of the spin state which governs the interface speed, $v \sim \sqrt{D_m}$. In the stationary and uniform state, that is, $^{\partial m}/_{\partial t} = 0$ and $\nabla^2 m = 0$, Equation (1) gives the self-consistent mean-field equation $m = \tanh[\beta(Jm - \Delta_{eff})]$, which leads, using the previous values, to a first-order transition with thermal hysteresis ranged between 107 K and 115 K (shown in Figure S7) approximately centered on the transition temperature $T_{eq} = \frac{2\Delta}{k_B \ln g} = 112.57$ K.

Equation (2) establishes the heat balance between the crystal and its environment. The first term, in the right-hand side, expresses the heat transfer from the crystal to the thermal bath (which is colder and maintained at temperature, $T_B = 105$ K $< T$), with a ratio $\alpha = 20$ s^{-1}. The second contribution contains the source term, $I(x,y,t)$, accounting for the deposited heat flow by the laser spot, in which $\rho = \frac{a_{HS}}{a_{LS}} = 0.51$ is the ratio between the HS and LS optical absorptions of the crystal, and $D_T = 200$ μm^2 s^{-1} is the thermal diffusion constant.

Equation (3) details the excitation intensity, which includes the homogeneous intensity of the microscope, $I_0 = 183$ K s^{-1} = 9.6 μW (specific intensity × crystal area), and that of the Gaussian-shaped-laser spot (size parameter, $\sigma = 12$ μm, located at coordinates $x_0 = 46$ μm; $y_0 = 10$ μm) the amplitude of which $\Delta I_{max} = 2.3$ mW is modulated at the frequency $\omega = 2.5$ rad s^{-1} ($\nu = 0.4$ Hz). Equations (1)–(3) are resolved using finite difference method for a rectangular 2D system of size $L_x \times L_y = 60$ μm × 20 μm (see Supporting Information for the details of the simulation). Initially (at time, $t = 0$, the laser is OFF), the interface is at rest (see panel 1 of Figure 3 a). When the laser is ON, the HS/LS interface performs periodic oscillations, as demonstrated in the selected snapshots of Figure 3 a. The complete spatiotemporal behavior of the system: interface position and temperature maps, is presented in movie S2.

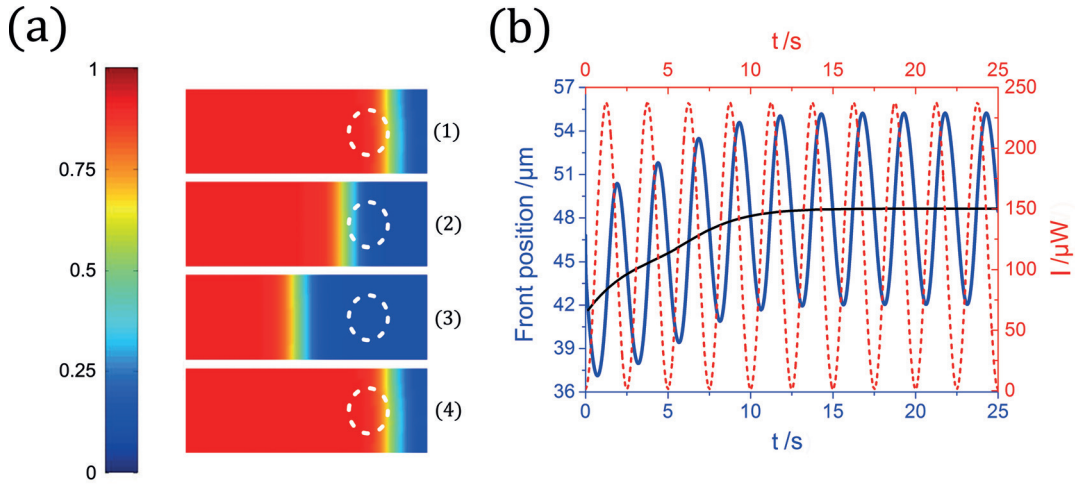

Figure 3. a): spatiotemporal model: snapshots (1)–(4) showing interface oscillations under light modulation recorded at times $t = 19.3$ s, 20 s, 20.6 s, and 21.8 s, respectively. The blue area corresponds to the LS phase the red area to the HS phase. Dashed white circles represent the laser spot. b) Computed time dependence of the excitation (dotted red line) and the HS/LS interface position (solid blue line). The black curve is the average position of the HS/LS interface.

In Figure 3b we plotted the calculated time dependence of the interface position and that of the light modulation. The results fairly reproduce the experimental observations of Figure 1c: 1) the interface responds with delay (the elliptic phase portrait is shown in Figure S8), and 2) it presents a global drift of its average position (black curve in Figure 3b). For a deeper understanding of the front control mechanism, we illustrated in Figure 4a the spatial profiles (along the direction of propagation), of the order-parameter n_{HS} and temperature (in red) at times: $t = 18.461$ s and $t = 19.291$ s (the corresponding laser intensities are 207.71 μW and 144.20 μW). The apparent correlation between the temperature and spin state curves is totally counter-intuitive and results from the photo-thermal history of the system. Note that at $t = 18.461$ s the region located at the right of the interface in the interval ($x = 42.5$–50 μm) is heated above T_{eq} ($= 112.57$ K); this triggers its switching into the HS phase, in accord with the reaction term of Equation (1), and drives the interface (Figure 4a; dashed blue curve) to the new position $x = 55$ μm at time $t = 19.29$ s. At this time, the temperature profile (Figure 4a; dashed red curve) has significantly decreased, owing to the exchange with thermal bath [Eq. (2)] and the motion will shortly stop. Clearly, the front control results from a subtle regulation of the temperature gradients by light inside the crystal and particularly around the HS/LS interface region.

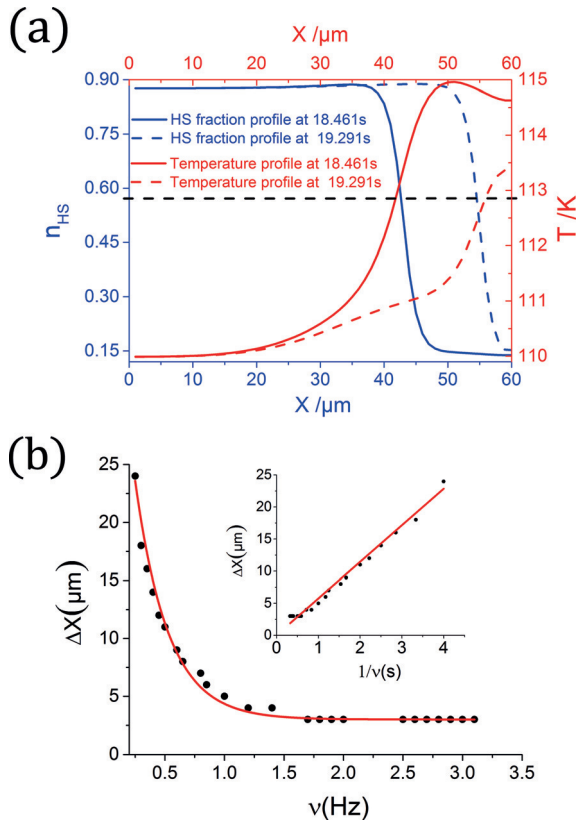

Figure 4. a) Spatial profiles of temperature (red) and high-spin fraction (blue) across the interface at $t = 18.461$ s (solid curves) and 19.291 s (dashed curves). The transition temperature is $T_{eq} \approx 112.6$ K (horizontal dashed black line). See main text for a detailed discussion. b) Displacement of the HS/LS interface as a function of the frequency of the light modulation. Solid lines are to guide the eye.

We also calculated the excursion amplitude of the HS/LS interface as a function of the excitation frequency. The results, summarized in Figure 4b, are remarkably consistent with the experiments. A cut-off frequency $\nu_c \approx 1.25$ s^{-1} is obtained and a linear plot was also found between ΔX_{max} and $1/\nu$. We could determine for the 1D system (see Supporting Information), the analytical expression of the cut-off frequency, $\nu_c = \frac{X_0^2}{4\pi D_T}$, where $X_0 \approx 50$ μm is the initial distance between the interface and the laser spot. Injecting the experimental value of ν_c, we estimated, for the first time, the thermal diffusion of the SC single crystal as $D_T = 300$ μm^{2}s^{-1}. This value is in excellent agreement with those measured for polymers,[24] $D_T = 250$ μm^{2}s^{-1}, which are expected to have similar mechanical and thermal characteristics to spin-crossover materials.

The substantial benefit of the current method compared to previous investigations using pulse laser excitations[25,26,30–34] lies in the reversible character of photo-control of the phase transition inside the thermal hysteresis, which can be monitored using a weak intensity of light. Note that bi-directional photo-switching inside the thermal hysteresis using pulsed nanosecond laser excitation was first reported for the SC sample [Fe(pyrazine)Pt(CN)$_4$],[35] and later on other type of SC solids,[36] using Raman spectroscopy. While there is no doubt about the physical mechanism of the LS to HS photo-transformation, the reverse process inside the hysteresis is still disputable. The reverse process feeds into the healthy debate, which was reignited recently by photo-calorimetric measurements[37] under pulse laser on the [Fe(pyrazine)Pt(CN)$_4$] SC sample, leading to a controversy. Of course, these results should be confirmed by other investigations, capitalizing as in Ref. [37], on the remarkable advances of the last two decades, in the chemical synthesis of high quality single crystals,[3,38–41] combined with technological advances in experimental techniques (ultra-fast photo-crystallography,[42–44] time-resolved optical experiments[27,45]), and methods of visualization at the nanoscale.[46]

In conclusion, we have experimentally shown that modulation of a weak intensity of light at a suitable frequency could reversibly control the spin transition in the thermal hysteresis interval. The reproducibility of oscillations of the HS/LS front even after several crystal cycling, during which the crystal maintained its integrity, suggests potential applications of SC solids in accurate actuation,[30] micro-positioning, and as switching devices. The existence of a cut-off frequency of about 1.5 Hz and the slow propagation velocity of the interface (at maximum 20 μm s^{-1} for thermally induced transformations) legitimately questions the possibility of ultra-fast reversible switching of cooperative SC materials at the macroscopic scale. However, recent studies using ultra-fast excitations[44] (on spin-crossover solids), showed multi-scale kinetics, in which the macroscopic HS fraction can be transformed at the speed of sound. Reducing the size may increase the interface velocity and enhance the resilience of the materials, the mechanical stress excess of which induced by the phase transition could be released more easily, benefiting from the favorable surface/volume ratio. Another important objective now is the synthesis of multifunctional ferroelectric–ferroelastic spin-crossover materials, which can lead to a remarkable piezoelectric (coupled with magnetic)

response, with numerous applications for actuators and sensors.

Acknowledgements

Acknowledgements are due to the University of Versailles, CNRS, and ANR agency (BISTA-MAT: ANR-12-BS07-0030-01) for their financial support. M.S. is grateful to the government of Sénégal and the French National Agency for Research (ANR) scholarships.

Keywords: elastic interface · optical microscopy · phase transition · spatio-temporal properties · spin-crossover

How to cite: *Angew. Chem. Int. Ed.* **2016**, *55*, 1755 – 1759
Angew. Chem. **2016**, *128*, 1787 – 1791

[1] "Spin crossover in iron(II)-complexes": P. Gütlich in *Metal Complexes*, Springer, Berlin, Heidelberg, **1981**, pp. 83 – 195.
[2] A. Hauser, *Coord. Chem. Rev.* **1991**, *111*, 275 – 290.
[3] "Spin-Crossover Materials: Properties and Applications": M. A. Halcrow, in *Spin-Crossover Materials*, Wiley, Hoboken, **2013**.
[4] P. Gütlich, H. A. Goodwin, *Spin Crossover in Transition Metal Compounds I – III*, Springer, Berlin Heidelberg, New York, **2004**.
[5] I. M. Miron, T. Moore, H. Szambolics, L. D. Buda-Prejbeanu, S. Auffret, B. Rodmacq, S. Pizzini, J. Vogel, M. Bonfim, A. Schuhl, G. Gaudin, *Nat. Mater.* **2011**, *10*, 419 – 423.
[6] L. Thomas, M. Hayashi, X. Jiang, R. Moriya, C. Rettner, S. S. P. Parkin, *Nature* **2006**, *443*, 197 – 200.
[7] T. A. Moore, P. Möhrke, L. Heyne, A. Kaldun, M. Kläui, D. Backes, J. Rhensius, L. J. Heyderman, J.-U. Thiele, G. Woltersdorf, A. Fraile Rodríguez, F. Nolting, T. O. Menteş, M. Á. Niño, A. Locatelli, A. Potenza, H. Marchetto, S. Cavill, S. S. Dhesi, *Phys. Rev. B* **2010**, *82*, 94445 – 94447.
[8] M. Sy, F. Varret, K. Boukheddaden, G. Bouchez, J. Marrot, S. Kawata, S. Kaizaki, *Angew. Chem. Int. Ed.* **2014**, *53*, 7539 – 7542; *Angew. Chem.* **2014**, *126*, 7669 – 7672.
[9] F. Varret, A. Slimani, K. Boukheddaden, C. Chong, H. Mishra, E. Collet, J. Haasnoot, S. Pillet, *New J. Chem.* **2011**, *35*, 2333 – 2340.
[10] C. Chong, A. Slimani, F. Varret, K. Boukheddaden, E. Collet, J.-C. Ameline, R. Bronisz, A. Hauser, *Chem. Phys. Lett.* **2011**, *504*, 29 – 33.
[11] W. Eerenstein, N. D. Mathur, J. F. Scott, *Nature* **2006**, *442*, 759 – 765.
[12] L. Keeney, T. Maity, M. Schmidt, A. Amann, N. Deepak, N. Petkov, S. Roy, M. E. Pemble, R. W. Whatmore, D. Johnson, *J. Am. Ceram. Soc.* **2013**, *96*, 2339 – 2357.
[13] D. M. Evans, A. Schilling, A. Kumar, D. Sanchez, N. Ortega, M. Arredondo, R. S. Katiyar, J. M. Gregg, J. F. Scott, *Nat. Commun.* **2013**, *4*, 1534.
[14] S.-I. Ohkoshi, H. Tokoro, T. Matsuda, H. Takahashi, H. Irie, K. Hashimoto, *Angew. Chem. Int. Ed.* **2007**, *46*, 3238 – 3241; *Angew. Chem.* **2007**, *119*, 3302 – 3305.
[15] P. N. Martinho, B. Gildea, M. M. Harris, T. Lemma, A. D. Naik, H. Müller-Bunz, T. E. Keyes, Y. Garcia, G. G. Morgan, *Angew. Chem. Int. Ed.* **2012**, *51*, 12597 – 12601; *Angew. Chem.* **2012**, *124*, 12765 – 12769.
[16] A. J. Fitzpatrick, E. Trzop, H. Muller-Bunz, M. M. Dirtu, Y. Garcia, E. Collet, G. G. Morgan, *Chem. Commun.* **2015**, *51*, 17540 – 17543.
[17] M. Zacharias, L. Bartosch, M. Garst, *Phys. Rev. Lett.* **2012**, *109*, 176401.
[18] A. Slimani, F. Varret, K. Boukheddaden, D. Garrot, H. Oubouchou, S. Kaizaki, *Phys. Rev. Lett.* **2013**, *110*, 087208.
[19] A. Slimani, F. Varret, K. Boukheddaden, C. Chong, H. Mishra, J. Haasnoot, S. Pillet, *Phys. Rev. B* **2011**, *84*, 094442.
[20] K. Nakano, N. Suemura, S. Kawata, A. Fuyuhiro, T. Yagi, S. Nasu, S. Morimoto, S. Kaizaki, *Dalton Trans.* **2004**, 982 – 988.
[21] C. J. Schneider, J. D. Cashion, B. Moubaraki, S. M. Neville, S. R. Batten, D. R. Turner, K. S. Murray, *Polyhedron* **2007**, *26*, 1764 – 1772.
[22] H. A. H. Al-Khazali, *IOSR J. Eng.* **2012**, *02*, 971 – 978.
[23] W. Braun, *Math. Ann.* **1875**, *8*, 567 – 573.
[24] O. Fouché, J. Degert, G. Jonusauskas, N. Daro, J. F. Létard, E. Freysz, *Phys. Chem. Chem. Phys.* **2010**, *12*, 3044 – 3052.
[25] Y. Ogawa, S. Koshihara, K. Koshino, T. Ogawa, C. Urano, H. Takagi, *Phys. Rev. Lett.* **2000**, *84*, 3181 – 3184.
[26] S. Bedoui, M. Lopes, S. Zheng, S. Bonnet, G. Molnar, A. Bousseksou, *Adv. Mater.* **2012**, *24*, 2475 – 2478.
[27] G. Gallé, D. Deldicque, J. Degert, T. Forestier, J. F. Létard, E. Freysz, *Appl. Phys. Lett.* **2010**, *96*, 041907.
[28] K. Boukheddaden, I. Shteto, B. Hôo, F. Varret, *Phys. Rev. B* **2000**, *62*, 14796 – 14805.
[29] K. Boukheddaden, M. Paez-Espejo, F. Varret, M. Sy, *Phys. Rev. B* **2014**, *89*, 224303.
[30] H. J. Shepherd, I. A. Gural'skiy, C. M. Quintero, S. Tricard, L. Salmon, G. Molnar, A. Bousseksou, *Nat. Commun.* **2013**, *4*, 2607.
[31] S. Bedoui, M. Lopes, W. Nicolazzi, S. Bonnet, S. Zheng, G. Molnar, A. Bousseksou, *Phys. Rev. Lett.* **2012**, *109*, 135702.
[32] S. Cobo, D. Ostrovskii, S. Bonhommeau, L. Vendier, G. Molnar, L. Salmon, K. Tanaka, A. Bousseksou, *J. Am. Chem. Soc.* **2008**, *130*, 9019 – 9024.
[33] E. Collet, L. Henry, L. Pineiro-Lopez, L. Toupet, J. A. Real, *Curr. Inorg. Chem.* **2015**, *5*, DOI: 10.2174/1877944105666150910233704.
[34] E. Collet, N. Moisan, C. Baldé, R. Bertoni, E. Trzop, C. Laulhé, M. Lorenc, M. Servol, H. Cailleau, A. Tissot, M.-L. Boillot, T. Graber, R. Henning, P. Coppens, M. B.-L. Cointe, *Phys. Chem. Chem. Phys.* **2012**, *14*, 6192 – 6199.
[35] S. Bonhommeau, G. Molnar, A. Galet, A. Zwick, J. A. Real, J. J. McGarvey, A. Bousseksou, *Angew. Chem. Int. Ed.* **2005**, *44*, 4069 – 4073; *Angew. Chem.* **2005**, *117*, 4137 – 4141.
[36] N. Ould Moussa, D. Ostrovskii, V. M. Garcia, G. Molnár, K. Tanaka, A. B. Gaspar, J. A. Real, A. Bousseksou, *Chem. Phys. Lett.* **2009**, *477*, 156 – 159.
[37] M. Castro, O. Roubeau, L. Piñeiro-López, J. A. Real, J. A. Rodríguez-Velamazán, *J. Phys. Chem. C* **2015**, *119*, 17334 – 17343.
[38] W. Bauer, M. M. DÎtru, Y. Garcia, B. Weber, *CrystEngComm* **2012**, *14*, 1223 – 1231.
[39] A. D. Naik, K. Robeyns, C. Meunier, A. Léonard, A. Rotaru, B. Tinant, Y. Filinchuk, B. L. Su, Y. Garcia, *Inorg. Chem.* **2014**, *53*, 1263 – 1265.
[40] See Ref. [15].
[41] P. Guionneau, *Dalton Trans.* **2014**, *43*, 382 – 393.
[42] M. Lorenc, C. Balde, W. Kaszub, A. Tissot, N. Moisan, M. Servol, M. Buron-Le Cointe, H. Cailleau, P. Chasle, P. Czarnecki, M. L. Boillot, E. Collet, *Phys. Rev. B* **2012**, *85*, 054302.
[43] A. Tissot, R. Bertoni, E. Collet, L. Toupet, M.-L. Boillot, *J. Mater. Chem.* **2011**, *21*, 18347.
[44] R. Bertoni, M. Lorenc, A. Tissot, M. L. Boillot, E. Collet, *Coord. Chem. Rev.* **2015**, *282 – 283*, 66 – 76.
[45] F. Guillaume, Y. A. Tobon, S. Bonhommeau, J.-F. Létard, L. Moulet, E. Freysz, *Chem. Phys. Lett.* **2014**, *604*, 105 – 109.
[46] R. M. van der Veen, O. H. Kwon, A. Tissot, A. Hauser, A. H. Zewail, *Nat. Chem.* **2013**, *5*, 395 – 402.

Received: October 5, 2015
Published online: January 6, 2016

